

## LIGHTNING NO<sub>x</sub> ESTIMATES FROM SPACE-BASED LIGHTNING IMAGERS

William J. Koshak\*

Earth Science Branch, NASA Marshall Space Flight Center, Huntsville, AL, USA

### 1. INTRODUCTION

The intense heating of air by a lightning channel, and subsequent rapid cooling, leads to the production of lightning nitrogen oxides (NO<sub>x</sub> = NO + NO<sub>2</sub>) as discussed in Chameides [1979]. In turn, the lightning nitrogen oxides (or "LNO<sub>x</sub>" for brevity) indirectly influences the Earth's climate because the LNO<sub>x</sub> molecules are important in controlling the concentration of ozone (O<sub>3</sub>) and hydroxyl radicals (OH) in the atmosphere [Huntrieser et al., 1998]. Climate is most sensitive to O<sub>3</sub> in the upper troposphere, and LNO<sub>x</sub> is the most important source of NO<sub>x</sub> in the upper troposphere at tropical and subtropical latitudes; hence, lightning is a useful parameter to monitor for climate assessments [Schumann and Huntrieser, 2007].

The National Climate Assessment (NCA) program was created in response to the Congressionally-mandated Global Change Research Act (GCRA) of 1990. Thirteen US government organizations participate in the NCA program which examines the effects of global change on the natural environment, human health and welfare, energy production and use, land and water resources, human social systems, transportation, agriculture, and biological diversity. The NCA focuses on natural and human-induced trends in global change, and projects major trends 25 to 100 years out.

In support of the NCA, the NASA Marshall Space Flight Center (MSFC) continues to assess lightning-climate inter-relationships [Koshak et al., 2015]. This activity applies a variety of NASA assets to monitor in detail the changes in both the characteristics of ground- and space- based lightning observations as they pertain to changes in climate. In particular, changes in lightning characteristics over the conterminous US (CONUS) continue to be examined by this author using data from the Tropical Rainfall Measuring

Mission Lightning Imaging Sensor (TRMM/LIS; Christian et al. [1999]; Cecil et al. [2014]).

In this study, preliminary estimates of LNO<sub>x</sub> trends derived from TRMM/LIS lightning optical energy observations in the 17 yr period 1998-2014 are provided. This represents an important first step in testing the ability to make remote retrievals of LNO<sub>x</sub> from a satellite-based lightning sensor. As is shown, the methodology can also be directly applied to more recently launched lightning mappers, such as the Geostationary Lightning Mapper (GLM; Goodman et al., [2013]), and the International Space Station LIS (ISS/LIS; Blakeslee and Koshak [2016]).

### 2. METHODOLOGY

The approach taken is to estimate the total production  $P$  of LNO<sub>x</sub> from (the low Earth orbiting) LIS as

$$P = \sum_{k=1}^{N_o} P_k + N_u \left( \frac{1}{N_o} \sum_{k=1}^{N_o} P_k \right). \quad (1)$$

Here,  $P_k$  is the LNO<sub>x</sub> production from the  $k^{\text{th}}$  flash observed by LIS, and  $N_o$  is the total number of flashes observed by LIS in a particular geographical region and period of interest. Because of the low Earth orbit, LIS will have a limited view-time of the geographical region during the period of interest, and LIS also has a flash detection efficiency below 100% that varies diurnally. Hence, these instrument characteristics can be used to infer the total flash count  $N$  for the region during the period (see Cecil et al. [2014] for additional details). The number of flashes undetected by LIS is then  $N_u = N - N_o$ . The second term in (1) is simply  $N_u$  times the LIS estimate of the mean production per flash.

A distinct advantage of GLM over TRMM/LIS and ISS/LIS is that it continuously monitors a region. Hence, the second term in (1), which is estimative, is not required for GLM.

Next, the LNO<sub>x</sub> production  $P_k$  from the  $k^{\text{th}}$  flash can be estimated from the detected optical energy.

---

\*Corresponding author: William J. Koshak, Earth Science Branch, NASA-MSFC, Mail Stop ST11, Bud Cramer Research Hall, 320 Sparkman Dr., Huntsville, AL 35805; e-mail: william.koshak@nasa.gov

One could consider using the optical energy incident on the sensor as was done in Koshak et al. (2014), but this quantity depends on three sensor parameters (i.e., orbit altitude, entrance pupil area, and bandwidth). To facilitate the inter-comparison of results derived from different sensors, it is beneficial to introduce a quantity  $\Gamma_\lambda$  that is invariant to these three sensor parameters, and is given by

$$\Gamma_\lambda \equiv \sum_{i=1}^m \sum_{j=1}^n \left[ \int_{2\pi} \cos \theta' \bar{\xi}_{\lambda ij} d\Omega' \right] a_j$$

$$\Rightarrow \Gamma_\lambda = \sum_{i=1}^m \sum_{j=1}^n \pi \bar{\xi}_{\lambda ij} a_j . \quad (2)$$

This is the entire cloud-top upward optical emission from a particular flash (the  $k$  subscript is dropped here for brevity). The flash illuminates a total of  $n$  pixels and spans a duration of  $m$  frames. So,  $\Gamma_\lambda$  is the sum of each upward emission associated with the  $j^{\text{th}}$  pixel footprint in each  $i^{\text{th}}$  frame. The pixel cloud-top footprint  $a_j$  emits a "spectral energy density"  $\bar{\xi}_{\lambda ij}$  (in units of  $\mu\text{J}/\text{m}^2/\text{sr}/\text{nm}$ ) that represents the radiant intensity integrated over one LIS charge coupled device (CCD) frame period ( $\sim 2$  ms); the overbar above this quantity in (2) refers to averaging over the pixel solid angle. The factor of  $\pi$  in (2) comes from the upper hemispherical solid angle integration shown and the assumption that the observed spectral energy density is emitted *isotropically* from each cloud-top footprint.

The estimate of LNOx  $P_k$  (in moles) from the  $k^{\text{th}}$  flash can then be written as

$$P_k = \frac{Y}{\beta N_A} \Gamma_{\lambda k} \Delta\lambda , \quad (3)$$

where  $Y \sim 10^{17}$  molecules per Joule is the NOx thermochemical yield (Borucki and Chameides, 1984),  $N_A = 6.022 \times 10^{23}$  molecules per mole is Avogadro's number,  $\Delta\lambda$  is the known sensor bandwidth (in nanometers), and  $\beta \sim 3.94 \times 10^{-11}$  is a dimensionless calibration scaling factor whose magnitude is chosen such that the mean LNOx per flash in the (arbitrarily selected) reference year 1998 is 250 moles/flash (i.e. a production value per flash commonly cited in the literature). The units of  $\Gamma_{\lambda k}$  used in (3) are Joules per nanometer.

### 3. COMPUTATION USING LIS DATA

An estimate of the mean spectral energy density incident on the LIS instrument is provided in the LIS event "radiance" data product, but the magnitude of this product has not been corrected to account for the angle-of-incidence to the lens. In other words, the amount of optical energy actually ingested by a pixel depends on several factors that change with incident boresight angle (i.e., lens system transmission, pixel quantum efficiency, entrance pupil diameter, bandwidth, and pixel solid angle). The net effect of the boresight dependence (i.e., roll-off of LIS sensitivity with increasing angle of incidence) has been quantified in the correction plot shown in Fig. 1 of Boccippio et al. (2002), but has not previously been applied. In order to improve the accuracy of results provided here, the correction has been implemented as follows

$$\bar{\xi}_{\lambda ij} = \frac{0.985 \zeta_{\lambda ij}}{F_j} , \quad (4)$$

where  $F_j$  is the correction factor ("roll-off" curve) associated with the  $j^{\text{th}}$  pixel of a given incidence angle, and was extracted from the Boccippio et al. (2002) study. For mid-range boresight angles, the value of  $F_j \sim 0.985$ ; i.e., midrange incidence has no net correction. The variable  $\zeta_{\lambda ij}$  is the spectral energy density value in the LIS event "radiance" data product.

Hence, for LIS, (4) is used to obtain the spectral energy densities required in the definition of  $\Gamma_\lambda$  so that the flash LNOx production in (3) can be estimated by LIS. The LIS data also provides the optical event footprint  $a_j$  needed in the  $\Gamma_\lambda$  calculation.

### 4. COMPUTATION USING GLM DATA

The GLM transient (lightning) optical amplitude calibration relates sensor digital count output to incident radiant optical energy (in Joules), rather than to a spectral energy density as done with LIS. Hence, the GLM digital count output that provides *incident* lightning optical energy  $q_{ij}$  values must be used to infer the associated incident spectral energy density. This is accomplished via the expression

$$\bar{\xi}_{\lambda ij} = \frac{q_{ij}}{A \Delta\omega_j \Delta\lambda} , \quad (5)$$

where  $A$  is the GLM entrance aperture area,  $\Delta\omega_j$  is the GLM pixel solid angle, and  $\Delta\lambda$  again represents the sensor bandwidth (for GLM in this case). Hence, (5) easily gives the values of the spectral energy densities that are needed in the  $\Gamma_\lambda$  calculation, and no correction is required for sensitivity roll-off with increasing boresight angle; i.e., the GLM design did not employ a wide-angle lens system as did the design of LIS.

The GLM and ISS/LIS are presently still under Post Launch Testing (PLT) validation with ongoing upgrades being made to the data products. Hence, the methodology presented here for making estimates of lightning optical energies and LNOx from these instruments will be applied at a later date.

## 5. RESULTS FOR TRMM/LIS

In support of the NCA program discussed in section 1, the above methodology for LIS was applied to analyze a 17 yr period (1998-2014) of TRMM/LIS data. The analysis region examined was the portion of the conterminous US (CONUS) covered by TRMM/LIS; i.e., up to about 38°N latitude.

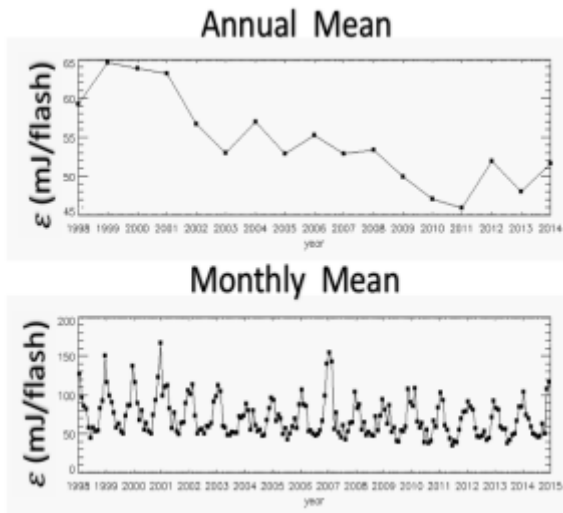


Fig. 1. The value of  $\epsilon$  (mJ/flash) derived from TRMM/LIS across the 17 yr period 1998-2014. Top plot is average optical energy per flash over a year, and bottom plot the average over a month. These "raw" results are only for flashes actually observed by TRMM/LIS.

The trend in the mean optical energy per flash  $\epsilon$  (in units of milliJoules per flash) was obtained by summing up the flash optical energy  $\Gamma_{\lambda k} \Delta\lambda$  for all  $k = 1, \dots, N_o$  flashes observed across the analysis region and then dividing by  $N_o$  to get the mean value for that period. Two analysis periods were

considered: annual, and monthly. The long-term trends of these quantities are provided in Fig. 1. Even though these plots implicitly assume isotropic emission in the calculation of the  $\Gamma_{\lambda k}$  values for each  $k^{\text{th}}$  flash, this is a minor point since each  $\Gamma_{\lambda k}$  value is still based on direct observations of the spectral energy density as shown in (2).

The associated trend in average LNOx production per flash  $\Lambda$  (in moles per flash) is estimated by using (1) and then dividing by  $N$ ; i.e.,  $\Lambda = P/N$ . The results are provided in Fig. 2. Again, both annual and monthly averaging periods are used. Whereas Fig. 1 shows results based only on direct observations of the  $N_o$  observed flashes in a period, the results in Fig. 2 attempt to account for the effects of all flashes  $N$ , where  $N = N_o + N_u$  as discussed in section 2.

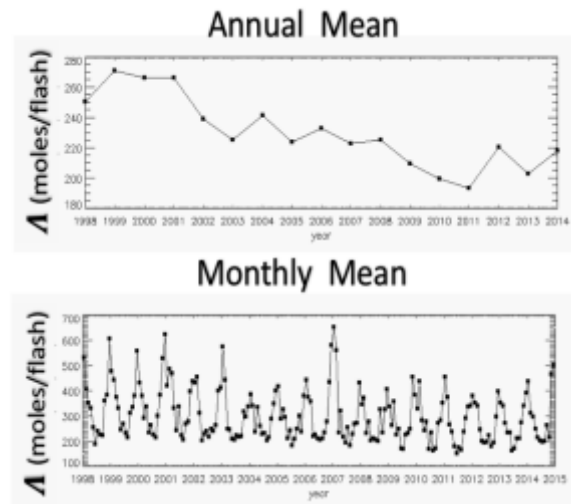


Fig. 2. The value of  $\Lambda$  (in moles/flash). These plots are based on the boosting of the "raw" (i.e. directly observed) flash count by the finite view-time and detection efficiency of the TRMM/LIS (see section 2 for details).

The total LNOx production obtained using (1) is provided in Fig. 3. Because the lightning flash count varies from year-to-year and from month-to-month, the LNOx production trends obviously depend on lightning frequency. Hence, whereas the plots in Figs. 1 and 2 are normalized with respect to flash count, the results in Fig. 3 are not. Normalizing with respect to flash count has the advantage of revealing how the typical LNOx production per flash varies over a long-term basis, and therefore is a more specific indicator of how the physics of individual flashes might be changing over time. By contrast, Fig. 3 shows net changes in LNOx production due to all flashes; i.e., the trend in total LNOx production depends not only

on the production per flash, but also on the flash count.

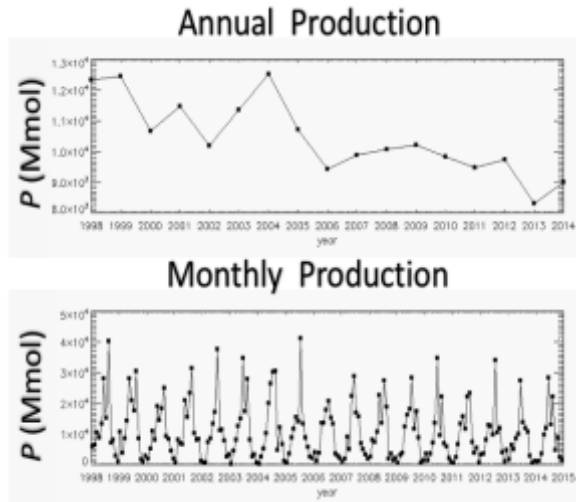


Fig. 3. The TRMM/LIS trend in total LNOx production  $P$  (in megamoles) as computed using (1). These plots depend not only on the variation of LNOx production per flash, but also on the flash count.

## 6. DISCUSSION

The first thing to note from the Annual Mean plots in Figs. 1 and 2 is that there is *not* a sharp (artificial) drop in energy and LNOx in going from year 2000 to 2001 due to the TRMM/LIS orbit altitude boost in August of 2001. That is, the higher the orbit altitude, the less energy will be incident on the sensor. Specifically, the incident lightning optical energy on TRMM/LIS changes from 909.1 fJ/flash (the average in 2000) down to 793.1 fJ/flash (the average in 2001), or a drop of 12.8%. The unit fJ here is femtojoules. Since the orbit altitude invariant quantity  $\Gamma_\lambda$  has been employed in this study instead of incident optical energy, the artificial drop (bias) due to increased orbit altitude has been avoided in the results of Figs. 1 and 2. Overall, there is a downward trend in optical energy and LNOx followed by an upward trend that starts in 2011.

Secondly, note the interesting cyclic pattern in the monthly trends of Figs. 1 and 2. The optical energy per flash peaks typically in January of each year, which might be indicative of a higher fraction of large current positive polarity cloud-to-ground lightning and/or smaller vertical cloud optical depths, as commonly associated with wintertime thunderstorms. In the monthly trends of Fig. 3, the maxima occur in the summer months because of high flash counts in the summer.

Finally, all the trend patterns provided in section 5 must be interpreted carefully. The

similarity in the trend patterns between Fig. 1 and Fig. 2 is because of the constant factor  $Y/(\beta N_A)$  that was assumed in the relationship between flash optical energy and flash LNOx production given in (3). In addition, as described above, the value of  $A = 250$  moles/flash in 1998 is a direct (intentional) consequence of the specific value chosen for  $\beta$  in order to reference or "calibrate" the overall plot trend to the widely-cited value of 250 moles/flash. For example, the value of  $\beta$  could be changed such that it forces the mean in 1998 to be some other value, say 500 moles/flash ... but the overall pattern of the trend (relative shape) would not be affected by this change. These nuances must always be kept in mind when interpreting the LNOx results provided here. In general, the value of  $\beta$  is not constant as assumed here, but rather depends on specific properties of the lightning channel, cloud optical scattering properties, and the instrument. So, the value of  $\beta$  technically changes from flash to flash. The accuracy of the method provided here clearly depends on how much the complicating fluctuations in  $\beta$  get "washed out" from statistical averaging over many flashes and cloud morphologies. In this respect, the annual trends shown here are likely more accurate than the monthly trends.

## 7. SUMMARY

A straight-forward methodology was provided that shows how one can attempt to estimate LNOx from an arbitrary satellite-based lightning imager (e.g., TRMM/LIS, ISS/LIS, or GLM). Flash LNOx production is estimated by first estimating the *total flash energy* from the observed flash optical energy emission. Multiplying the total flash energy by a NOx thermochemical yield and dividing by Avogadro's number converts the total flash energy into LNOx production in units of moles.

The observed cloud-top lightning optical energy is a tiny fraction of the total flash energy, and this tiny fraction varies from flash to flash. However, on a statistical basis (i.e., over many flashes and many cloud morphologies) one can infer the value of this tiny fraction that is needed in order to produce a reasonable average LNOx production per flash, such as 250 moles/flash. This is the basic approach taken in this writing. Therefore, the trends in LNOx per flash found in this study should be interpreted carefully, and represent relative trends only.

There are several improvements provided in this study over that provided in Koshak et al. (2014). First, an upward spectral energy  $\Gamma_\lambda$  was

employed to describe the flash optical emission, and this approach removes sensor biases (such as the effects of sensor orbit altitude, or sensor entrance pupil area). Second, TRMM/LIS lightning optical energy amplitudes were corrected for sensor sensitivity roll-off with boresight angle. Third, in addition to the standard annual mean trends, long term trends of *monthly* mean LNO<sub>x</sub> per flash were provided here. These trends show interesting cycles across each year, with maxima in mean LNO<sub>x</sub>/flash occurring in January. Fourth, the trending of TRMM/LIS LNO<sub>x</sub> production in this study was extended to one additional year, resulting in a total analysis period of 17 yrs (1998-2014).

In the future, the method provided here will also be used to estimate LNO<sub>x</sub> production from ISS/LIS and GLM datasets after post-launch testing of these instruments is completed.

*Acknowledgments.* This work was supported by NASA Headquarters program announcement number NNH14ZDA001N-INCA under Dr. Jack Kaye and Dr. Lucia Tsaoussi in support of the National Climate Assessment program.

## 8. REFERENCES

Blakeslee, R. J., and W. J. Koshak, 2016: LIS on ISS: expanded global coverage and enhanced applications, *The Earth Observer*, Volume 28, Issue 3, May-June.

Boccippio, D. J., W. J. Koshak, R. J. Blakeslee, 2002: Performance assessment of the Optical Transient Detector and Lightning Imaging Sensor. Part I: predicted diurnal variability, *J. Atmos. Oceanic Technol.*, 19, 1318-1332.

Borucki, W. J., and W. L. Chameides, 1984: Lightning: estimates of the rates of energy dissipation and nitrogen fixation, *Rev. Geophys. Space Phys.*, 22, 363-372.

Cecil, D. J., D. E. Buechler, and R. J. Blakeslee, 2014: Gridded lightning climatology from TRMM-LIS and OTD: dataset description, *Atmos. Res.*, 135 -136, 404 - 414.

Chameides, W. L., 1979: Effect of variable energy input on nitrogen fixation in instantaneous linear discharges, *Nature*, 277, 123-125.

Christian, H. J., et al., 1999: The Lightning Imaging Sensor, in *11th Int. Conf. on Atmospheric Electricity*, pp. 746-749, ICAE, Guntersville, AL.

Goodman, S. J., et al., 2013: The GOES-R Geostationary Lightning Mapper (GLM), *Atmos. Res.*, 125-126, 34-49.

Huntrieser, H., H. Schlager, C. Feigl, and H. Holler, 1998: Transport and production of NO<sub>x</sub> in electrified thunderstorms: Survey of previous studies and new observations at midlatitudes, *J. Geophys. Res.*, 103, 28,247-28,264.

Koshak, W. J., B. Vant-Hull, E. W. McCaul, and H. S. Peterson, 2014: Variation of a lightning NO<sub>x</sub> indicator for National Climate Assessment, *XV International Conference on Atmospheric Electricity*, Norman, Oklahoma, June 15-20.

Koshak, W. J., K. L. Cummins, D. E. Buechler, B. Vant-Hull, R. J. Blakeslee, E. R. Williams, H. S. Peterson, 2015: Variability of CONUS Lightning in 2003-12 and Associated Impacts, *J. Appl. Meteorol. Climatology*, 54, No. 1, 15-41.

Schumann, U., and H. Huntrieser, 2007: The global lightning-induced nitrogen oxides source, *Atmos. Chem. Phys.*, 7, 3823-3907.